Electronic Supplementary Material (ESI) for Physical Chemistry Chemical Physics.

Internal dynamics in helical molecules studied by X-ray diffraction, NMR spectroscopy and DFT calculations

Martin Dračínský,*[a] Jan Storch,[b] Vladimír Církva,[b] Ivana Císařová,[c] Jan Sýkora*[b]

[a]*Institute of Organic Chemistry and Biochemistry, Czech Academy of Sciences, Flemingovo 2, 16610 Prague, Czech Republic. E-mail: dracinsky@uochb.cas.cz*
[b]*Institute of Chemical Process Fundamentals, Czech Academy of Sciences, Rozvojová 135, 16502 Prague, Czech Republic. E-mail: sykora@icpf.cas.cz*
[c]*Faculty of Science, Charles University in Prague, Hlavova 2030, 12840 Prague, Czech Republic.*

Electronic Supplementary Information

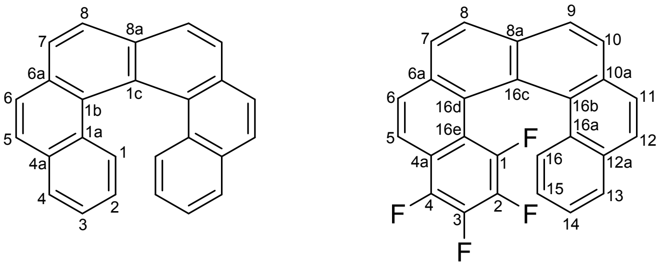

Figure S1. The atom numbering used for [6]helicene and tetrafluoro[6]helicene throughout the manuscript except for the calculations of ring puckering parameters (see below).

X-Ray

Table S1. The variable temperature X-ray structure analysis performed on [6]helicene

Temperature (K)	100	150	300
Unit cell dimmensions (Å)	7.3058(2)	7.3280(3)	7.3417(3)
	12.9470(5)	13.0400(6)	13.1529(4)
	17.4452(6)	17.4490(5)	17.5885(5)
Volume (Å^3)	1650.11(10)	1667.38(11)	1698.43(10)
Final R, wR	00331, 0.0810	0.0345, 0.0795	0.0392, 0.0800
Goodness of fit	0.9382	1.0363	0.9820
Largest diff. peak and hole (e/Å^3)	0.24, -0.20	0.15, -0.13	0.11, -0.17

The ring puckering parameters according to Cremer and Pople, the total puckering amplitude Q and angles θ and Φ,[37] were calculated in program PARST97.[36] The parameters for right-handed helicenes are listed in Table S2. The atom numbering reflects the ortho-condensation of aromatic rings and starts with the inner quarternary carbon (Figure S2). As Ag-[6]helicene complex, [6]helicene-perfluorobenzene complex and tetrafluoro[6]helicene crystallize in centrosymmetric space groups, both enantiomers (P and M type) are present in these structures. Although [6]helicene crystallizes in the space group $P2_12_12_1$ that requires only one enantiomer, the crystal structure contains both enantiomers due to lamellar twinning. The magnitude of parameter Q indicates the degree of distortion, the higher Q the larger distortion. The angles θ and Φ characterise the shape of the conformation. Northern hemisphere is defined by the angle θ within the range 0–90° and southern hemisphere is defined by θ in the range of 90–180°. The angle Φ localizes the conformation within the given hemisphere. All the conformations of the right-handed helicenes (type P) are located in the southern hemisphere within narrow range of conformations between $^{2}T_{4}$ – $B_{4,1}$ – $^{3}T_{1}$ close to the ´equator´ (Figure S3a). The most distorted central rings 3 and 4 are concentrated in the range $^{2}T_{4}$ – $B_{4,1}$. The rings 2 and 5 are less distorted and adopt the conformation close to $B_{4,1}$. While the conformations of almost planar peripheral rings 1 and 6 can be localized near the $^{3}T_{1}$ conformation. The conformations of individual aromatic rings in left-handed helicene molecules can be found in the centrosymmetric positions in the northern hemisphere (Figure S3b).

Table S2. List of ring puckering parameters

Ring number	[6]helicene			Ag^+ - [6]helicene			F_4 - [6]helicene		
	Q(Å)	θ (°)	Φ (°)	Q(Å)	θ (°)	Φ (°)	Q(Å)	θ (°)	Φ (
1	0.035	105.7	160.9	0.059	102.1	136.0	0.065	114.1	182.
2	0.139	104.4	166.0	0.108	110.6	180.0	0.156	108.2	192.
3	0.193	109.0	198.0	0.195	108.6	187.8	0.194	109.3	200.
4	0.195	110.8	200.7	0.213	106.3	189.1	0.185	110.7	196.
5	0.157	106.5	173.2	0.117	101.4	147.8	0.141	108.7	183.
6	0.041	102.1	142.5	0.008	92.0	190.0	0.057	102.6	163.

Ring number	F_6Ph - [6]helicene			TMA - [6]helicene		
	Q(Å)	θ (°)	Φ (°)	Q(Å)	θ (°)	Φ (°)
1	0.059	107.5	150.3	0.066	102.8	170.9
2	0.140	107.5	184.3	0.115	111.0	188.0
3	0.184	110.3	198.6	0.180	108.3	198.4

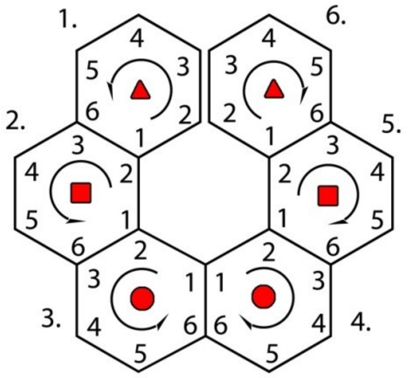

Figure S2. The atom and ring numbering used in the calculation of ring puckering parameters.

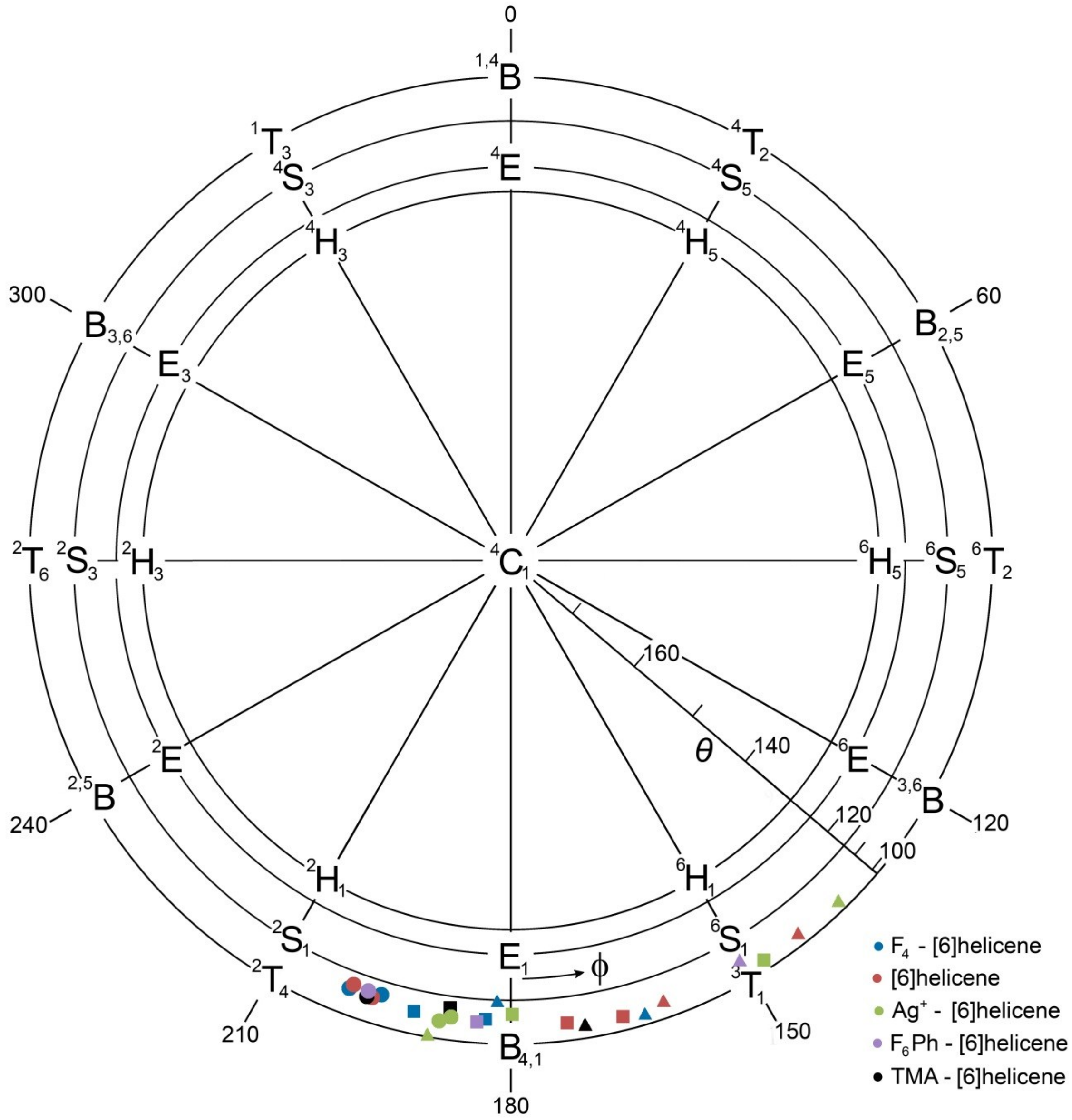

Figure S3a. Ring puckering parameters of individual aromatic rings in right-handed helicenes (projection for a uniform value of total puckering amplitude *Q*); B = boat, C = chair, E = envelope, H = half-chair, S = screw-boat.

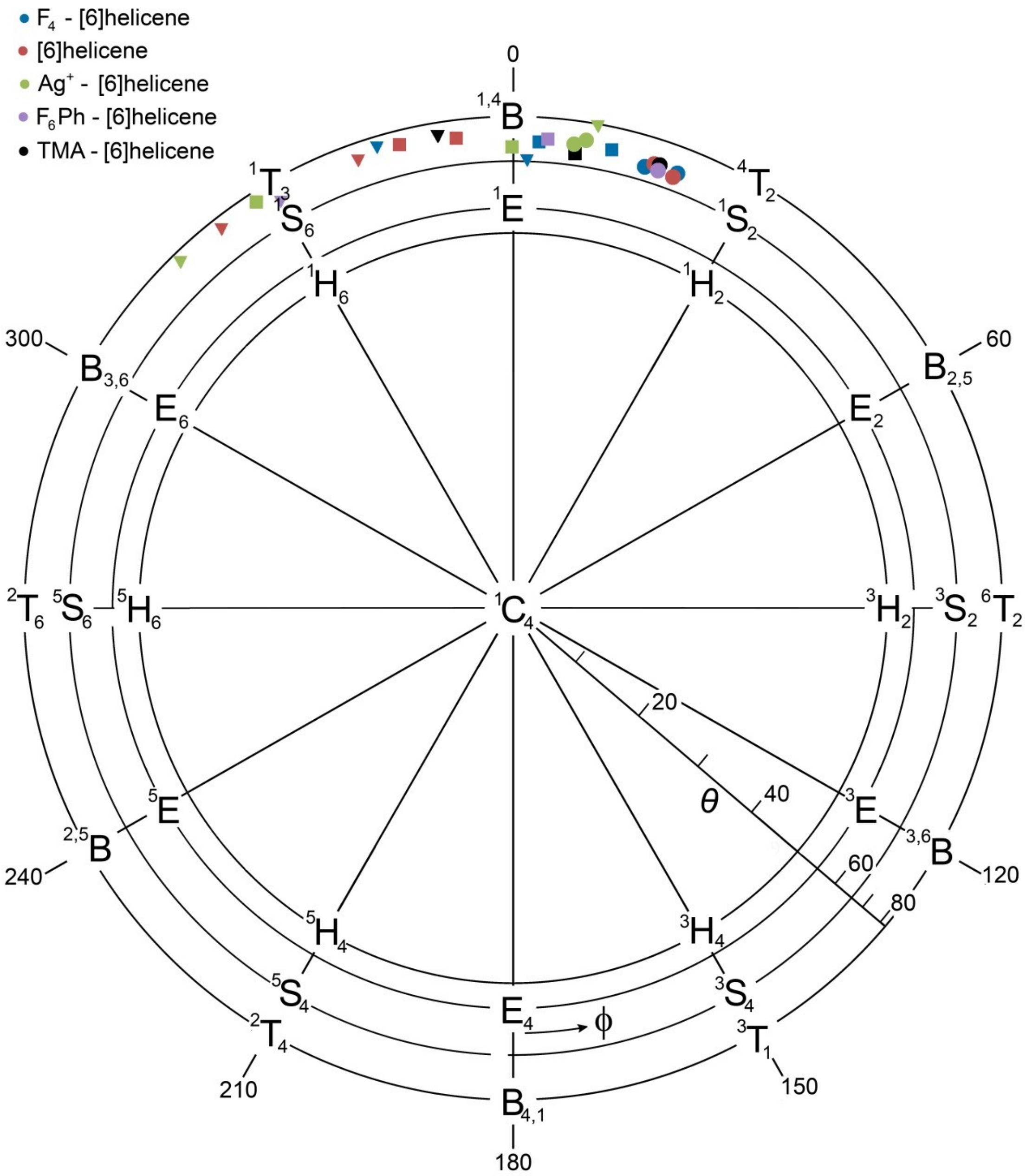

Figure S3b. Ring puckering parameters of individual aromatic rings in letf-handed helicenes (projection for a uniform value of total puckering amplitude *Q*); B = boat, C = chair, E = envelope, H = half-chair, S = screw-boat.

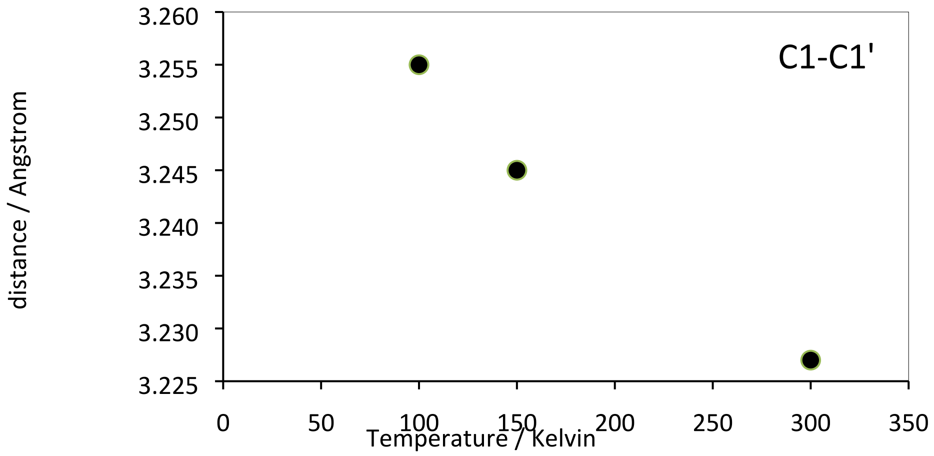

a)

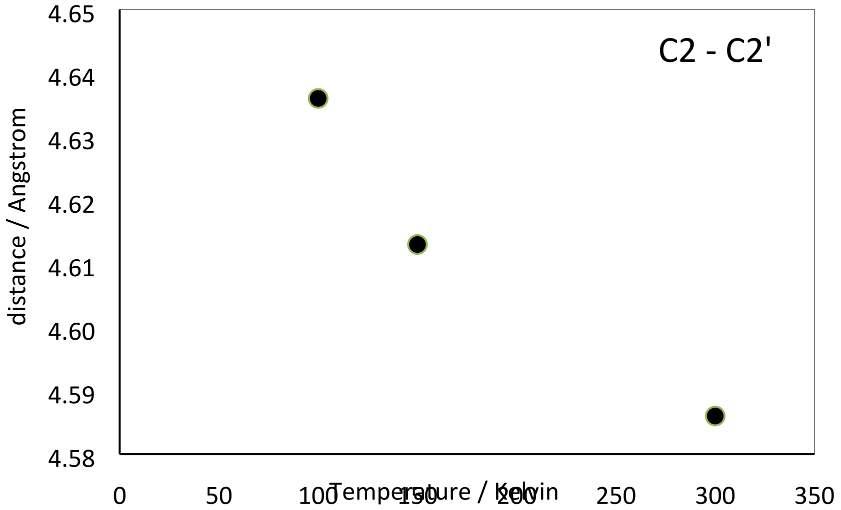

b)

Figure S4. Shrinking of the distance between peripheral rings with elevated temperature; a) distance C1-C1’, b) distance C2-C2’.

NMR spectroscopy

Table S3. Experimental ^{1}H and ^{13}C chemical shifts and chemical shift differences of the terminal benzene ring of [6]helicene and tetrafluoro[6]helicene. For complete signal assignment and atom numbering see below.

	Exp DMSO	298K
	[6]helicene	**F4-[6]helicene**
H1	7.43	7.01
H2	6.68	6.80
H3	7.26	7.37
H4	7.94	8.00
C1	126.75	125.31
C2	124.97	124.33
C3	125.98	126.05
C4	128.08	128.11
C4a	131.63	132.15
C1a	129.32	127.64

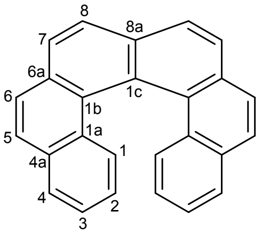

^{13}C NMR (DMSO-d_6, 125.7 MHz, 298 K): δ (ppm) 131.63 (C4a), 131.14 (C6a), 130.01 (C8a), 129.32 (C1a), 128.24 (C5), 128.08 (C4), 127.65 (C7), 127.27 (C1b), 127.23 (C8), 126.75 (C1), 126.47 (C6), 125.98 (C3), 124.97 (C2), 123.17 (C1c). ^{1}H NMR (DMSO-d_6, 499.9 MHz, 298 K): δ (ppm) 8.18 (H8), 8.15 (H7), 8.10 (H6), 8.06 (H5), 7.94 (H4), 7.43 (H1), 7.26 (H3), 6.68 (H2).

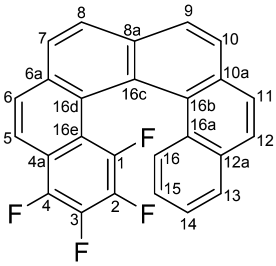

^{13}C NMR (DMSO-d_6, 125.7 MHz, 298 K): δ (ppm) 143.06 (C1), 141.85 (C4), 137.76 (C2), 136.91 (C3), 132.67 (C8a), 132.17 (C12a), 131.92 (C6a), 130.29 (C10a), 129.52 (C6), 129.46 (C8), 128.52 (C10), 128.31 (C12), 128.26 (C16b), 128.13 (C13), 127.65 (C16a), 126.98 (C7), 126.46 (C9), 126.42 (C11), 126.07 (C14), 125.33 (C16), 124.35 (C15), 123.82 (C16c), 121.37 (C16d), 118.13 (C5), 117.41 (C4a), 117.06 (C16e). ^{1}H NMR (DMSO-d_6, 499.9 MHz, 298 K): δ (ppm) 8.39 (H8), 8.36 (H6), 8.29 (H7), 8.27 (H5), 8.22 (H10, 8.22 (H9), 8.11 (H11), 8.09 (H12), 8.00 (H13), 7.37 (H14), 7.01 (H16), 6.80 (H15). ^{19}F NMR (DMSO-d_6, 470.3 MHz, 298 K): δ (ppm) -129.25 (F1), -149.24 (F4), -159.87 (F3), -161.20 (F3).

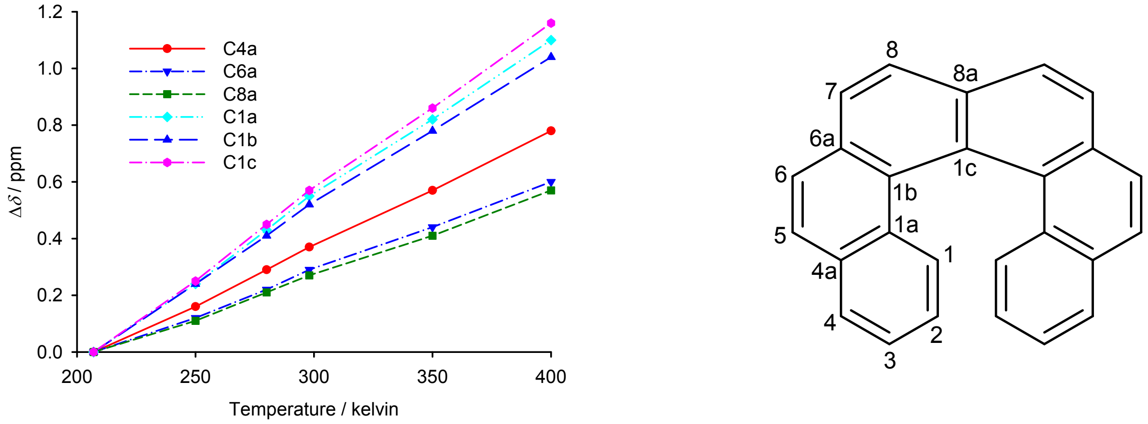

Figure S5. Temperature dependence of relative chemical shifts of quaternary carbon atoms in [6]helicene with respect to C8. Quaternary and CH carbons are depicted in separate figures because vibrational averaging of chemical shifts at different temperatures may be significantly different for these atoms.[49]

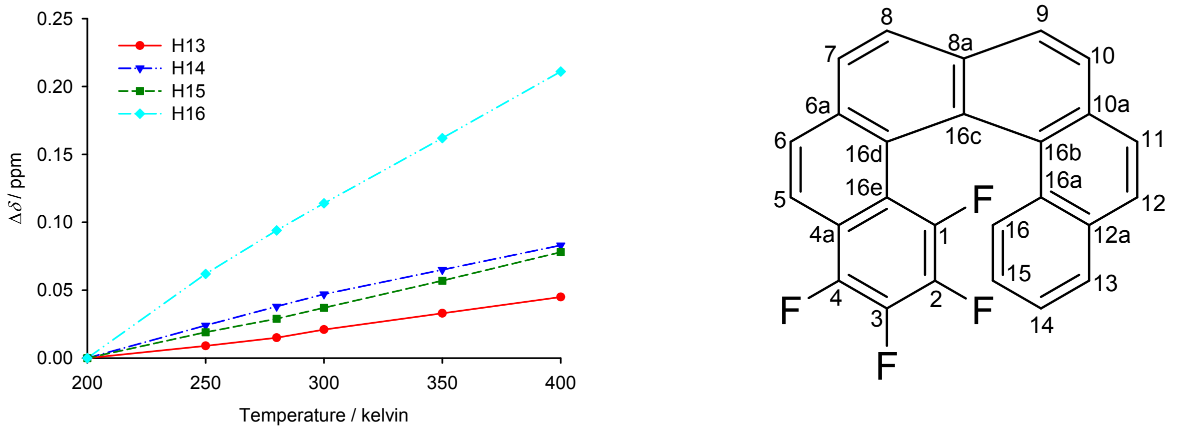

Figure S6. Temperature dependence of relative chemical shifts of hydrogen atoms in tetrafluoro[6]helicene with respect to the chemical shift of H8.

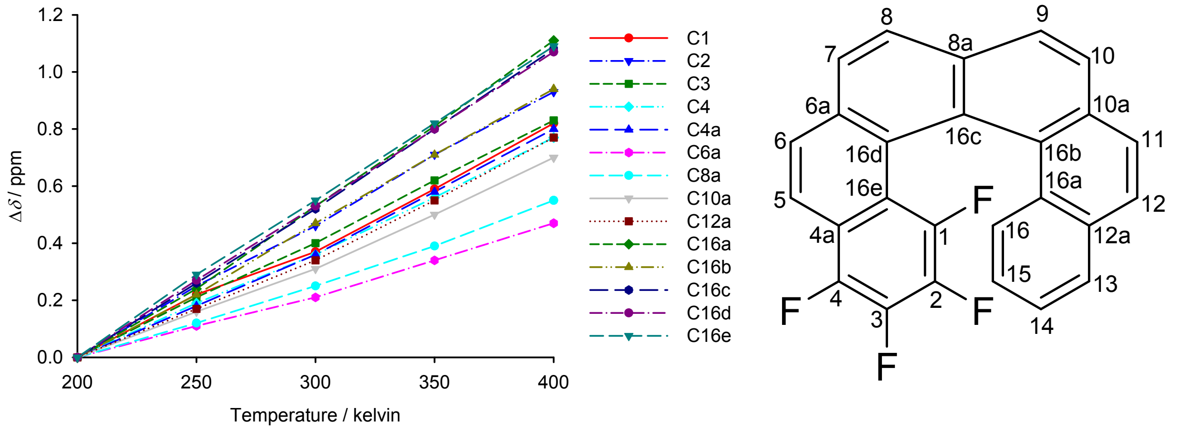

Figure S7. Temperature dependence of relative chemical shifts of quaternary carbon atoms in tetrafluoro[6]helicene with respect to the chemical shift of C8.

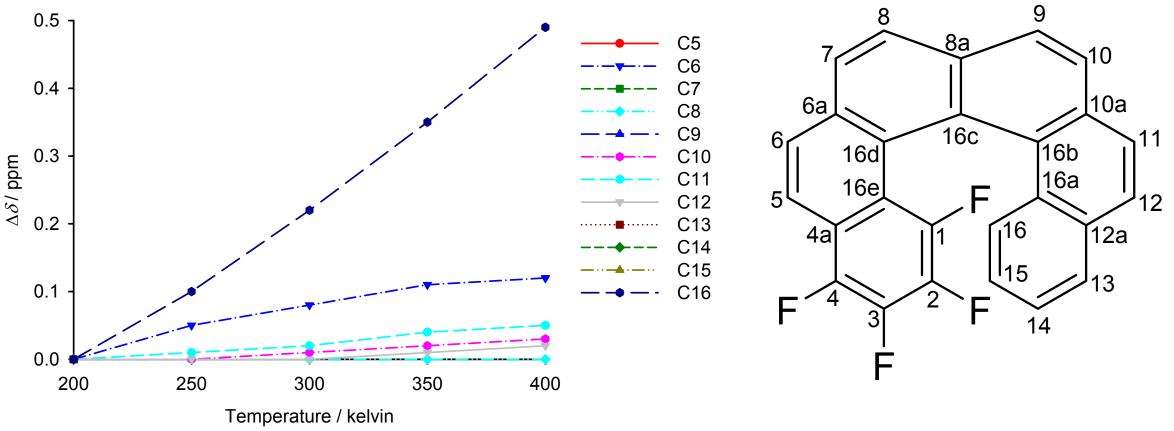

Figure S8. Temperature dependence of relative chemical shifts of CH carbon atoms in tetrafluoro[6]helicene with respect to the chemical shift of C8.

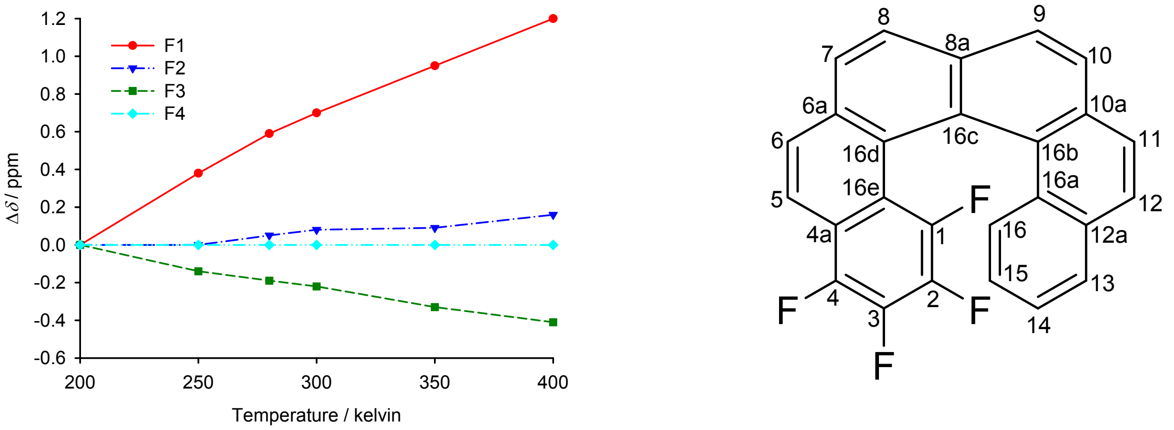

Figure S9. Temperature dependence of relative chemical shifts of fluorine atoms in tetrafluoro[6]helicene with respect to F4.

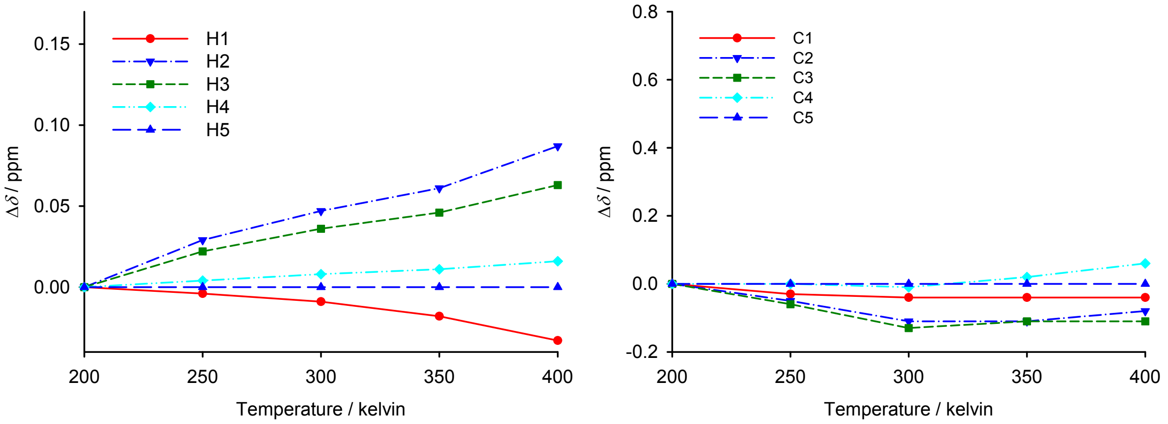

Figure S10. The temperature dependence of relative ^{1}H chemical shifts with respect to H5 (left) and ^{13}C chemical shifts with respect to C5 (right) in phenanthrene measured in acetone and DMSO. The *y* axis scaling is identical to that in Figure 4 in the main text.

DFT calculations

To further investigate the influence of the computational method on the molecular geometry, the structures of [6]helicene and tetrafluoro[6]helicene optimized with PBE functional are compared to those optimized with the popular hybrid functional B3LYP and the influence of the basis set and the method for empirical correction for dispersion on the geometry was also determined. These calculations were performed in Gaussian program, because hybrid functionals are computationally very expansive with plane-wave basis sets used in CASTEP.[51] The calculations without dispersion correction lead to slightly longer C2–C2' distance (by 0.04 Å) with B3LYP functional (Table S3). However, these differences are cancelled in optimizations with dispersion correction. Adding diffusion functions also slightly increases C2–C2' distance, while polarization functions have a negligible effect. Dispersion corrections significantly reduce C2–C2' distance in the optimized structures (by 0.2–0.3 Å) with a larger effect of the D2 version[52] of the Grimme's correction than the D3 version.[53] At all computational levels, C2–C2' distance in tetrafluoro[6]helicene is shorter by ca 0.2 Å.

Table S4. The C2–C2' distance (Angstrom) in isolated structures of [6]helicene and tetrafluoro[6]helicene optimized at different levels of theory.

Compound	Dispersion correction	PBE	PBE	PBE	B3LYP	B3LYP	B3LYP
		6-31g	6-31g(d,p)	6-311+g(d,p)	6-31g	6-31g(d,p)	6-311+g(d,p)
[6]helicene	no	4.400	4.399	4.431	4.438	4.436	4.474
	GD2	4.229	4.224	4.245	4.226	4.218	4.246
	GD3	4.286	4.283	4.307	4.287	4.281	4.312
F4-[6]helicene	No	4.280	4.287	4.311	4.328	4.337	4.373
	GD2	4.038	4.040	4.057	4.030	4.033	4.067
	GD3	4.130	4.135	4.152	4.126	4.132	4.168

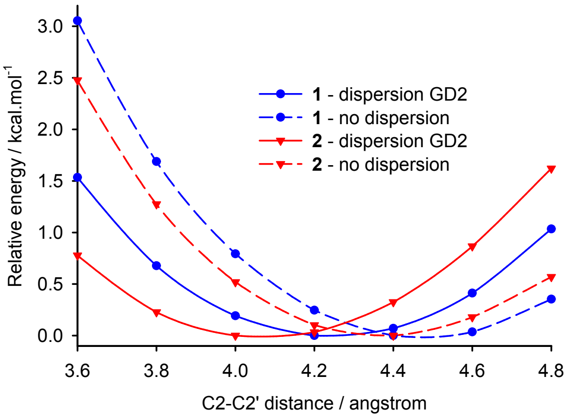

Figure S11. The calculated (B3LYP/6-311+G**, with and without dispersion correction D2) dependence of relative energy of [6]helicene and tetrafluoro[6]helicene on the C2–C2' distance.